

Wavelet-Driven 3D Anomaly Detection with Pose-Agnostic and Sparse-View Supplementary Materials

Mingwen Shao^{1,2} Qiao Zhang^{2*} Xinyuan Chen² Xiang Lv² Lingzhuang Meng²
Chang Liu² Qinglin Zhan² Ling Jian³

¹ Artificial Intelligence Research Institute, Shenzhen University of Advanced Technology

² Shandong Key Laboratory of Intelligent Oil & Gas Industrial Software, Qingdao Institute of Software, College of Computer Science and Technology, China University of Petroleum (East China)

³ School of Economics and Management, China University of Petroleum (East China)

smw278@126.com, bz24070008@s.upc.edu.cn, b24070011@s.upc.edu.cn, lvxiang1997@126.com,
lzhmeng1688@163.com, upc_liuchang@163.com, s24070001@s.upc.edu.cn, bebetter@upc.edu.cn

Overview

The supplementary material presents the following sections to strengthen the main manuscript:

Sec. A shows more ablation studies.

Sec. B shows more quantitative comparisons.

Sec. C shows more qualitative comparisons.

A. Ablation Study

Table 5 presents the per-category ablation results on the PIAD_synt (20%) dataset, evaluating the effectiveness of each proposed component: SWGM (Structure-aware Wavelet-optimized Gaussian Modeling), WPE (Wavelet-based Pose Estimator), and WDAD (Wavelet Difference-aware Anomaly Detector). Compared to the full model ("All"), the removal of any single component results in a performance decline in both pixel-level and image-level AUROC. Notably, the absence of WPE causes the most substantial drop, reducing the mean image-level AUROC from 82.34 to 78.65, underscoring the critical importance of Wavelet-based matching verification and pose optimization in addressing sparse-view challenges. The complete model consistently outperforms others across most object categories, highlighting the synergistic contributions of all three components.

B. Quantitative Comparison

Quantitative comparison of each category on MAD_sim.

Table 1 and Table 2 report the per-category performance of Wave-Pose3D and three state-of-the-art PAD methods (OmniPoseAD [3], SplatPose [1], and PIAD [2]) on the MAD_sim dataset under 10% and 20% sparse-view settings,

respectively. Across both configurations, our method consistently achieves the highest average AUROC at both pixel and image levels. Specifically, Wave-Pose3D attains a mean pixel-level AUROC of 94.0 and 95.1 under 10% and 20% settings, outperforming PIAD by 1.6% and 2.1%, respectively. At the image level, our approach yields 64.6 and 69.1 average AUROC, showing clear improvements over the best-performing baseline PIAD (60.2 and 64.5). Notably, our method achieves the highest scores in the majority of object categories (e.g., Gorilla, Pig, Bear, Scorpion), demonstrating its robustness in both fine-grained anomaly localization and holistic detection, even under severe view sparsity.

Quantitative comparison of each category on PIAD_synt. Table 3 and Table 4 show per-category results on the PIAD_synt dataset under 10% and 20% sparse-view settings. Across both configurations, Wave-Pose3D consistently outperforms OmniPoseAD, SplatPose, and PIAD on both pixel-level and image-level AUROC. At 10% sparsity, our method achieves a mean pixel AUROC of 96.3 and image AUROC of 73.2, surpassing the best baseline (PIAD) by 1.1% and 5.8%, respectively. When increasing to 20% views, Wave-Pose3D further improves to 97.8 (pixel) and 82.3 (image), ranking first in most categories and demonstrating strong robustness and generalization under limited view conditions.

C. Qualitative comparison

Figure 1 shows a qualitative comparison with PIAD in a 20% sparse setting. It can be seen that our method can predict more accurate poses, reconstruct accurate and anomaly-free objects, and ultimately obtain precise positioning results.

*Corresponding author

Objects	P_AUROC				LAUROC			
	OmniPoseAD (NeurIPS23)	SplatPose (CVPRW24)	PIAD (CVPR25)	Wave-Pose3D Ours	OmniPoseAD (NeurIPS23)	SplatPose (CVPRW24)	PIAD (CVPR25)	Wave-Pose3D Ours
01Gorilla	88.1	91.1	92.5	95.2	51.9	53.9	50.2	57.7
02Unicorn	90.2	90.8	92.6	95.5	52.6	52.5	53.4	69.4
03Mallard	92.1	91.2	93.3	94.4	59.2	62.2	64.2	65.6
04Turtle	91.2	90.8	91.0	92.4	55.5	53.7	59.4	66.1
05Whale	88.6	89.2	92.0	93.6	59.3	63.8	66.0	58.9
06Bird	89.4	91.1	92.5	93.4	51.4	56.7	53.8	59.8
07Owl	91.2	92.3	94.1	94.7	55.6	56.2	56.6	64.4
08Sabertooth	91.5	91.8	91.0	93.7	54.3	58.6	61.9	54.5
09Swan	85.4	88.1	92.3	96.4	55.6	61.3	62.7	69.8
10Sheep	94.3	93.7	94.9	94.2	65.3	62.8	62.3	67.7
11Pig	91.6	93.7	95.0	95.9	59.7	52.6	61.9	65.5
12Zalika	87.3	89.6	90.5	93.6	60.5	64.9	64.7	66.8
13Pheonix	85.7	90.5	94.2	92.4	57.6	59.7	62.4	63.1
14Elephant	83.1	81.2	83.9	87.5	62.4	61.9	64.2	67.1
15Parrot	86.2	89.2	90.0	94.4	61.3	62.6	65.3	59.8
16Cat	89.6	91.4	95.5	95.1	56.3	57.4	57.5	70.3
17Scorpion	88.2	87.6	89.9	91.8	51.6	53.4	62.4	65.8
18Obesobeso	90.2	91.6	96.3	94.2	52.3	54.6	62.3	68.4
19Bear	89.6	91.2	94.6	95.8	60.3	62.9	62.3	67.7
20Puppy	88.2	89.1	90.9	94.9	57.2	56.8	52.1	63.4
Mean	89.1	90.3	92.4	94.0	57.0	58.4	60.2	64.6

Table 1. Quantitative comparison of each category on the MAD_sim (10%) dataset. The best performance is highlighted in **bold**, while the second-best is underlined.

Objects	P_AUROC				LAUROC			
	OmniPoseAD (NeurIPS23)	SplatPose (CVPRW24)	PIAD (CVPR25)	Wave-Pose3D Ours	OmniPoseAD (NeurIPS23)	SplatPose (CVPRW24)	PIAD (CVPR25)	Wave-Pose3D Ours
01Gorilla	88.3	92.1	93.5	96.4	56.9	55.4	57.6	68.6
02Unicorn	91.2	90.8	91.7	96.3	57.6	53.2	56.8	76.7
03Mallard	93.4	93.2	95.1	94.6	63.2	64.3	67.6	68.2
04Turtle	91.2	90.8	91.0	93.5	56.5	54.4	59.4	68.2
05Whale	89.4	91.2	93.0	93.4	59.3	65.4	73.7	66.3
06Bird	90.2	92.1	93.2	95.3	58.4	60.3	59.1	62.8
07Owl	93.6	92.3	94.9	96.6	55.6	54.2	58.5	65.7
08Sabertooth	92.5	91.8	93.4	93.6	56.3	59.7	73.3	61.8
09Swan	86.4	90.1	92.2	95.5	59.6	62.3	65.6	71.2
10Sheep	95.3	96.7	97.3	97.2	65.3	68.5	71.2	71.6
11Pig	90.6	93.7	95.7	96.7	59.7	54.2	61.3	68.7
12Zalika	88.6	89.6	91.0	94.0	60.5	62.9	71.1	68.4
13Pheonix	86.2	90.5	92.9	93.2	59.6	58.3	64.8	65.5
14Elephant	85.1	83.2	85.1	90.8	62.4	61.2	67.5	70.0
15Parrot	87.4	90.2	92.3	94.7	64.3	65.3	66.8	66.4
16Cat	90.6	93.4	96.3	97.7	60.3	58.3	63.2	70.7
17Scorpion	89.6	87.6	89.9	93.7	53.6	54.9	62.4	77.7
18Obesobeso	91.6	92.6	96.3	97.2	57.6	56.3	68.1	74.4
19Bear	92.6	91.2	94.6	97.1	65.3	68.5	64.0	70.8
20Puppy	90.1	89.3	91.3	94.0	61.2	62.3	57.6	68.6
Mean	90.2	91.1	93.0	95.1	59.7	60.0	64.5	69.1

Table 2. Quantitative comparison of each category on the PIAD_synt (10%) dataset. The best performance is highlighted in **bold**, while the second-best is underlined.

References

- [1] Mathis Kruse, Marco Rudolph, Dominik Woiwode, and Bodo Rosenhahn. Splatpose & detect: Pose-agnostic 3d anomaly detection. In *Proceedings of the IEEE/CVF Conference on Computer Vision and Pattern Recognition*, pages 3950–3960, 2024. 1
- [2] Kaichen Yang, Junjie Cao, Zeyu Bai, Zhixun Su, and Andrea Tagliasacchi. Piad: Pose and illumination agnostic anomaly detection. In *Proceedings of the Computer Vision and Pattern Recognition Conference*, pages 4734–4743, 2025. 1
- [3] Qiang Zhou, Weize Li, Lihan Jiang, Guoliang Wang, Guyue Zhou, Shanghang Zhang, and Hao Zhao. Pad: A dataset and

benchmark for pose-agnostic anomaly detection. *Advances in Neural Information Processing Systems*, 36:44558–44571, 2023. 1

Objects	P_AUROC				LAUROC			
	OmniPoseAD (NeurIPS23)	SplatPose (CVPRW24)	PIAD (CVPR25)	Wave-Pose3D Ours	OmniPoseAD (NeurIPS23)	SplatPose (CVPRW24)	PIAD (CVPR25)	Wave-Pose3D Ours
Axletree	94.3	96.4	<u>97.0</u>	98.2	64.4	68.8	<u>73.7</u>	80.2
Box	92.8	<u>94.3</u>	95.7	95.7	<u>63.2</u>	62.3	<u>52.3</u>	63.7
Can	96	<u>96.5</u>	<u>97.9</u>	98.9	74.5	73.4	<u>84.0</u>	86.0
Chain	96.8	<u>98.0</u>	<u>97.9</u>	98.2	62.4	61.2	67.6	<u>64.6</u>
Gear	93.4	<u>94.3</u>	<u>93.4</u>	93.7	57.4	65.4	70.4	<u>65.3</u>
Keyring	96.5	97.8	<u>98.8</u>	98.9	68.3	71.2	70.3	76.2
Motor	<u>89.7</u>	87.8	<u>85.8</u>	91.6	50.2	<u>54.3</u>	52.3	64.6
Parts	<u>94.3</u>	93.3	<u>94.6</u>	94.8	53.9	51.2	<u>60.2</u>	68.7
Picker	<u>94.3</u>	93.2	<u>94.1</u>	94.5	54.6	56.9	<u>59.9</u>	65.5
Section	<u>92.6</u>	96.5	<u>98.8</u>	99.1	69.9	73.4	<u>80.7</u>	85.2
Shaft	91.3	95.4	<u>98.0</u>	98.5	58.7	64.3	<u>63.0</u>	77.9
Spray_can	91.1	98.7	<u>99.2</u>	99.4	96.5	95.6	<u>99.1</u>	99.3
Spring	90.9	94.5	<u>95.9</u>	97.9	70.7	73.2	<u>77.0</u>	80.7
Sprockets	89.7	<u>92.6</u>	<u>91.4</u>	93.3	50.4	58.7	<u>65.2</u>	78.8
Amphora	87.6	<u>90.2</u>	92.5	<u>92.3</u>	48.9	<u>65.4</u>	<u>54.6</u>	57.1
Teapot	90.2	91.1	<u>92.1</u>	94.4	45.6	<u>49.9</u>	48.6	57.9
Mean	92.6	94.4	95.2	96.3	61.9	65.3	67.4	73.2

Table 3. Quantitative comparison of each category on the PIAD_synt (10%) dataset. The best performance is highlighted in **bold**, while the second-best is underlined.

Objects	P_AUROC				LAUROC			
	OmniPoseAD (NeurIPS23)	SplatPose (CVPRW24)	PIAD (CVPR25)	Wave-Pose3D Ours	OmniPoseAD (NeurIPS23)	SplatPose (CVPRW24)	PIAD (CVPR25)	Wave-Pose3D Ours
Axletree	95.2	96.3	98.3	98.7	67.6	78.8	83.0	84.3
Box	94.1	94.4	96.5	99.0	63.4	65.4	58.9	81.7
Can	96.6	97.6	98.9	99.1	89.2	92.5	93.5	93.1
Chain	96.2	97.8	98.2	98.3	65.4	67.8	75.8	72.6
Gear	91.4	92.1	94.3	94.8	78.8	81.1	88.5	90.3
Keyring	95.4	97.1	98.9	99.2	68.7	71.2	83.5	80.8
Motor	90.1	91.2	90.6	96.8	61.3	63.2	67.8	79.6
Parts	94.4	95.5	95.2	97.6	62.6	58.9	68.0	82.2
Picker	91.2	92.3	94.9	96.9	63.0	53.2	61.0	75.3
Section	96.4	97.5	98.9	99.3	75.6	77.7	82.1	92.5
Shaft	94.3	97.3	98.9	98.6	76.5	78.2	88.4	79.5
Spray_can	97.6	98.9	99.2	99.5	95.6	97.8	99.1	99.4
Spring	94.3	97.4	98.9	98.8	71.0	72.2	77.6	83.8
Sprockets	91.2	93.9	93.9	97.2	67.5	69.8	75.5	89.0
Amphora	91.2	92.1	93.5	94.8	52.3	54.3	57.9	62.0
Teapot	91.3	91.4	92.8	95.4	56.7	54.1	45.5	71.4
Mean	93.8	95.3	96.4	97.8	69.7	71.0	75.4	82.3

Table 4. Quantitative comparison of each category on the PIAD_synt (20%) dataset. The best performance is highlighted in **bold**, while the second-best is underlined.

Object	Baseline		w/o SWGM		w/o WPE		w/o WDAD		All	
	Axletree	97.3	77.0	98.7	84.0	98.4	82.5	98.7	84.9	98.7
Box	96.7	62.1	98.6	81.1	98.2	66.3	98.5	80.0	99.0	81.7
Can	98.1	81.7	99.1	90.5	99.1	86.6	98.8	91.9	99.1	93.1
Chain	97.6	70.4	98.3	72.8	98.7	86.3	98.2	72.7	98.3	72.6
Gear	94.2	74.9	94.7	83.4	94.7	80.5	94.2	85.2	94.8	90.3
Keyring	97.7	74.6	99.1	77.6	99.3	85.4	99.1	74.1	99.2	80.8
Motor	92.1	64.7	96.9	74.7	96.3	74.4	96.8	74.4	96.8	79.6
Parts	95.7	60.1	97.7	79.0	97.4	79.7	97.8	78.1	97.6	82.2
Picker	94.6	55.8	96.9	70.3	97.2	73.0	96.9	68.5	96.9	75.3
Section	97.5	85.9	99.2	87.7	99.2	86.3	99.1	89.9	99.3	92.5
Shaft	97.1	76.4	98.6	76.0	98.5	80.2	98.6	84.3	98.6	79.5
Spray_can	98.4	99.1	99.4	99.3	99.5	99.6	99.3	99.3	99.5	99.4
Spring	97.2	75.8	98.1	81.7	98.8	86.5	99.0	77.8	98.8	83.8
Sprockets	94.9	77.5	96.4	84.9	96.3	83.7	97.2	87.7	97.2	89.0
Amphora	93.2	61.8	95.1	58.3	95.0	57.6	94.4	61.1	94.8	62.0
Teapot	91.9	52.4	96.3	64.4	93.6	49.9	95.8	73.3	95.4	71.4
Mean	95.89	71.89	97.69	80.05	97.51	78.65	97.65	80.2	97.75	82.34

Table 5. Ablation study on PIAD_synt (20%) with per-category results of the proposed components. The best performance is highlighted in **bold**.

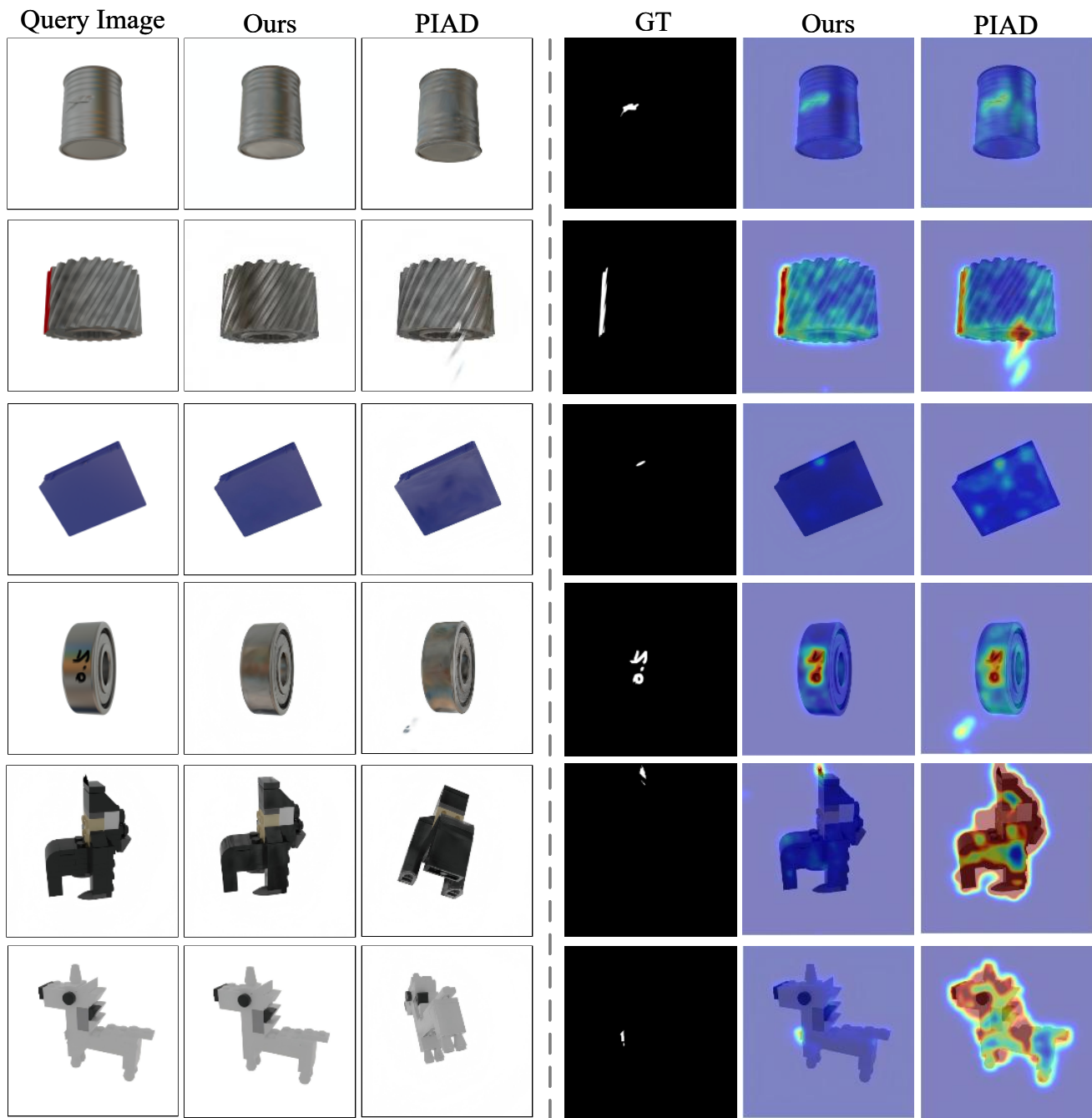


Figure 1. Qualitative visualization of pixel-wise anomaly segmentation compared to the state-of-the-art method PIAD in the 20% sparse view setting. The left side compares the rendered images produced by our method and baselines, while the right side visualizes the corresponding anomaly segmentation results.